



plants



Article

Blue Photons from Broad-Spectrum LEDs Control Growth, Morphology, and Coloration of Indoor Hydroponic Red-Leaf Lettuce

Qingwu Meng and Erik S. Runkle

Special Issue

The Effects of LED Light Spectra and Intensities on Plant Growth 2.0

Edited by

Dr. Valeria Cavallaro and Dr. Rosario Muleo



Article

Blue Photons from Broad-Spectrum LEDs Control Growth, Morphology, and Coloration of Indoor Hydroponic Red-Leaf Lettuce

Qingwu Meng ^{1,*}  and Erik S. Runkle ^{2,*} 

¹ Department of Plant and Soil Sciences, University of Delaware, 531 South College Avenue, Newark, DE 19716, USA

² Department of Horticulture, Michigan State University, 1066 Bogue Street, East Lansing, MI 48824, USA

* Correspondence: qwmeng@udel.edu (Q.M.); runkleer@msu.edu (E.S.R.)

Abstract: For indoor crop production, blue + red light-emitting diodes (LEDs) have high photosynthetic efficacy but create pink or purple hues unsuitable for workers to inspect crops. Adding green light to blue + red light forms a broad spectrum (white light), which is created by: phosphor-converted blue LEDs that cast photons with longer wavelengths, or a combination of blue, green, and red LEDs. A broad spectrum typically has a lower energy efficiency than dichromatic blue + red light but increases color rendering and creates a visually pleasing work environment. Lettuce growth depends on the interactions of blue and green light, but it is not clear how phosphor-converted broad spectra, with or without supplemental blue and red light, influence crop growth and quality. We grew red-leaf lettuce ‘Rouxai’ in an indoor deep-flow hydroponic system at 22 °C air temperature and ambient CO₂. Upon germination, plants received six LED treatments delivering different blue fractions (from 7% to 35%) but the same total photon flux density (400 to 799 nm) of 180 μmol·m⁻²·s⁻¹ under a 20 h photoperiod. The six LED treatments were: (1) warm white (WW₁₈₀); (2) mint white (MW₁₈₀); (3) MW₁₀₀ + blue₁₀ + red₇₀; (4) blue₂₀ + green₆₀ + red₁₀₀; (5) MW₁₀₀ + blue₅₀ + red₃₀; and (6) blue₆₀ + green₆₀ + red₆₀. Subscripts denote photon flux densities in μmol·m⁻²·s⁻¹. Treatments 3 and 4 had similar blue, green, and red photon flux densities, as did treatments 5 and 6. At the harvest of mature plants, lettuce biomass, morphology, and color were similar under WW₁₈₀ and MW₁₈₀, which had different green and red fractions but similar blue fractions. As the blue fraction in broad spectra increased, shoot fresh mass, shoot dry mass, leaf number, leaf size, and plant diameter generally decreased and red leaf coloration intensified. Compared to blue + green + red LEDs, white LEDs supplemented with blue + red LEDs had similar effects on lettuce when they delivered similar blue, green, and red photon flux densities. We conclude that the blue photon flux density in broad spectra predominantly controls lettuce biomass, morphology, and coloration.

Keywords: indoor vertical farming; green light; red light; sole-source lighting; white light



Citation: Meng, Q.; Runkle, E.S. Blue Photons from Broad-Spectrum LEDs Control Growth, Morphology, and Coloration of Indoor Hydroponic Red-Leaf Lettuce. *Plants* **2023**, *12*, 1127. <https://doi.org/10.3390/plants12051127>

Academic Editors: Valeria Cavallaro and Rosario Muleo

Received: 7 February 2023

Revised: 21 February 2023

Accepted: 22 February 2023

Published: 2 March 2023



Copyright: © 2023 by the authors. Licensee MDPI, Basel, Switzerland. This article is an open access article distributed under the terms and conditions of the Creative Commons Attribution (CC BY) license (<https://creativecommons.org/licenses/by/4.0/>).

1. Introduction

Photons with wavelengths between 400 and 750 nm are essential to plant growth and development by driving photosynthetic activity, regulating morphological adaption, and modulating secondary metabolism. This wavelength range is typically divided into four 100 nm wavebands: blue (400 to 499 nm), green (500 to 599 nm), red (600 to 699 nm), and far red (700 to 750 nm). Photosynthesis is wavelength-dependent as these photons carry energy that differentially excites two photosystems in plant cell membranes in light-dependent reactions of photosynthesis [1,2]. Although the traditionally defined photosynthetically active radiation (400 to 700 nm) only includes blue, green, and red light, recent research has shown the equal efficacy of supplemental far-red light in whole-plant photosynthesis [2–4]. Moreover, light mediates plant morphological responses by controlling photoreceptors. Blue light is absorbed by photoreceptors including cryptochrome 1, cryptochrome 2, and

phototropins [5], whereas red and far-red light are primarily absorbed by members in the phytochrome family [6]. Both cryptochromes and phytochromes can absorb green light, albeit poorly [7]. Increasing the fraction of blue photons relative to green or red photons generally decreases indoor-grown lettuce extension growth and biomass accumulation but increases pigmentation, whereas increasing the fraction of far-red photons generally does the opposite by eliciting the shade avoidance response [8–10].

In the last decade, lighting for controlled-environment agriculture has evolved rapidly thanks to the improved energy efficiency, spectral tuning, and design of light-emitting diode (LED) fixtures. These improvements increased the commercial adoption of LED fixtures, especially in indoor vertical farms. Growers can choose from a wide range of LED fixtures with different specifications. The selection depends, in part, on the fixture cost, photosynthetic photon efficacy (the photosynthetic photon output per unit energy in $\mu\text{mol}\cdot\text{J}^{-1}$), photon spectrum, form factor, and light responses of crops [11]. Although blue + red LEDs are prevalent in horticultural applications primarily because of their high photon and photosynthetic efficacy [11,12], there are merits to broad-spectrum LEDs. The addition of green light to blue + red light creates white light to the human eye but decreases the photosynthetic photon efficacy [13]. Unlike blue + red LEDs, which create pink or purple hues, broad-spectrum LEDs can reveal the true colors of plants, which facilitates workers' inspection of crop growth, nutrient conditions, insects, and diseases in a visually pleasing environment. High color fidelity under broad-spectrum LED lighting can be especially desirable in indoor vertical farms.

Although combining monochromatic blue, green, and red LEDs can create white light, commercial white LEDs are typically blue LEDs with a phosphor coating that converts most of the blue photons to photons at longer wavelengths (i.e., green, red, and far red), thereby emitting a broad range of biologically active radiation [13]. Depending on the material and amount of phosphor coatings, white LEDs create different hues, as indicated by the correlated color temperature (CCT). With a low percentage of blue light (e.g., 7%), warm-white LEDs have a low CCT of 2500 to 3500 K, whereas neutral-white (3500 to 4500 K), cool-white (4500 to 5500 K), and daylight (5500 to 7500 K) LEDs have higher percentages of blue light (e.g., 20% and 30%, respectively) and higher photon efficacies [11,14]. These white LEDs also differ in how they reveal the true colors of plants, as indicated by the color rendering index (CRI, negative to 100) or the TM-30 fidelity index (R_f , 0 to 100), with higher indices indicating higher color fidelity. Other specialized white LEDs also exist, such as mint-white (also known as equalized-white) LEDs. Developed by OSRAM Opto Semiconductors, these are blue LEDs with an efficient green phosphor coating that can be combined with red LEDs to create high-CRI white light [15].

Horticultural lighting companies often supplement white LEDs with monochromatic blue and/or red LEDs to create distinct broad spectra. First, this allows for spectrum customization to elicit specific plant responses (e.g., high yield, compact growth, and increased production of secondary metabolites) [16]. Second, including more efficient blue (peak wavelength ≈ 450 nm) and/or red (peak wavelength ≈ 660 nm) LEDs increases fixture photosynthetic photon efficacy while still providing acceptable color rendering at a low cost [15]. From an energy efficiency standpoint, warm-white (CCT = 2700 K) and cool-white (CCT = 6500 K) LEDs have lower photon efficacies (2.6 and $2.9 \mu\text{mol}\cdot\text{J}^{-1}$, respectively) than blue, red, and far-red LEDs (3.5 , 4.5 , and $4.7 \mu\text{mol}\cdot\text{J}^{-1}$, respectively) [11]. However, the overall performance of LED fixtures and light use efficiency of plants depend on both photosynthetic photon efficacy and crop responses under different photon spectra. While it is straightforward to compare cost and efficacy of lighting fixtures, there is little information about how indoor leafy greens grow under phosphor-converted broad spectra, with and without supplemental blue (peak wavelength ≈ 450 nm) + red (peak wavelength ≈ 660 nm) LEDs, relative to monochromatic blue + green (peak wavelength ≈ 525 nm) + red LEDs. Therefore, the objective of this study was to characterize the growth responses of hydroponic red-leaf lettuce (*Lactuca sativa*) 'Rouxai' under sole-source LED lighting with various broad spectra, sometimes with matching waveband-integrated photon flux densities. We

hypothesized the broad spectra with higher ratios of blue to green or red light would lead to lower lettuce biomass, decreased extension growth, and greater red leaf coloration.

2. Results

2.1. Biomass and Morphology

Lettuce shoot fresh mass was greatest under WW_{180} , MW_{180} , and $B_{20}G_{60}R_{100}$, and lowest under $MW_{100}B_{50}R_{30}$ and $B_{60}G_{60}R_{60}$ (Figure 1). Shoot dry mass showed a similar response as shoot fresh mass. Plants grew similarly under WW_{180} and MW_{180} with 78–98% and 39–62% higher shoot fresh and dry mass, respectively, than those that grew similarly under $MW_{100}B_{50}R_{30}$ and $B_{60}G_{60}R_{60}$. Compared to WW_{180} , shoot fresh and dry mass was 14% lower under $MW_{100}B_{10}R_{70}$, but similar under $B_{20}G_{60}R_{100}$. Plants developed approximately three fewer leaves when grown under $MW_{100}B_{50}R_{30}$ and $B_{60}G_{60}R_{60}$ than the other treatments. Plant biomass corresponded to leaf and plant size; the treatment trends were similar for shoot dry mass and plant diameter. Likewise, the leaves were longest and widest for the plants grown under WW_{180} and MW_{180} and shortest and narrowest for the plants grown under $MW_{100}B_{50}R_{30}$ and $B_{60}G_{60}R_{60}$. Leaf length and width were 17–19% and 25–35% greater, respectively, under WW_{180} and MW_{180} than $MW_{100}B_{50}R_{30}$ and $B_{60}G_{60}R_{60}$.

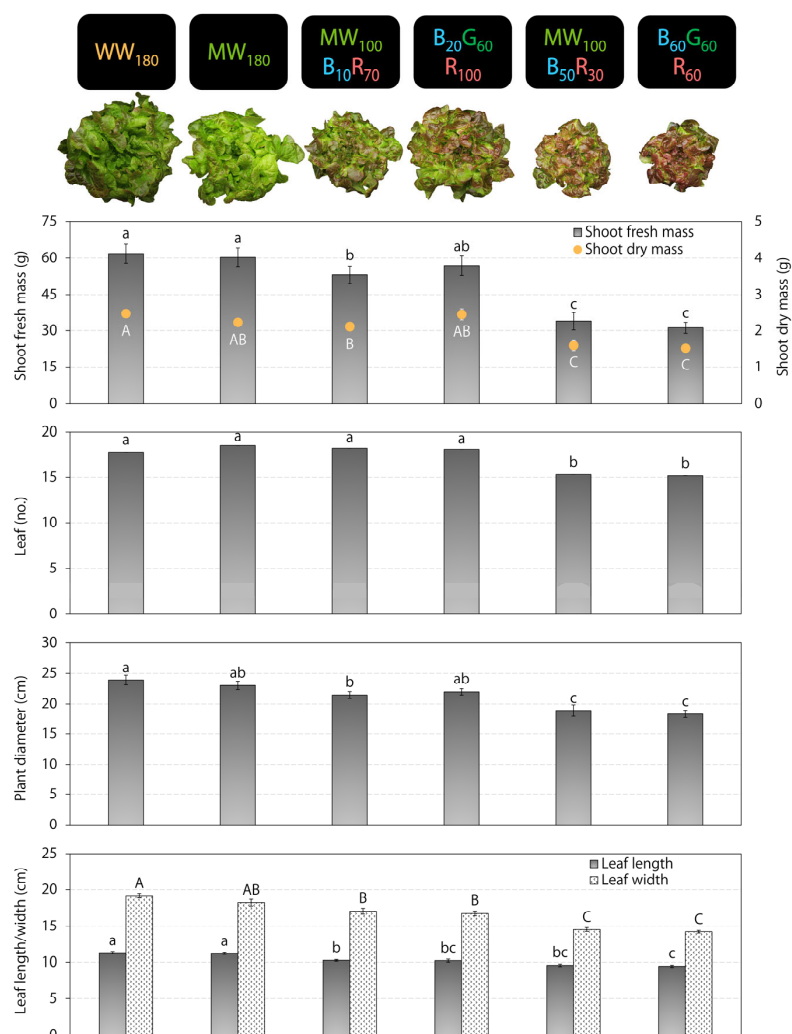


Figure 1. Shoot fresh and dry mass, leaf number, plant diameter, and length and width of the sixth most mature true leaf of red-leaf lettuce ‘Rouxai’ grown under six indoor lighting treatments delivered by warm-white (WW), mint-white (MW), blue (B), green (G), and/or red (R) light-emitting diodes (LEDs) ($n = 20$). The number after each LED type is its photon flux density in $\mu\text{mol}\cdot\text{m}^{-2}\cdot\text{s}^{-1}$. For each parameter, values followed by different letters are statistically different ($\alpha = 0.05$).

2.2. Coloration

Plants grown under WW_{180} and MW_{180} were visually greener with little red coloration, whereas those grown under the other treatments had distinct foliage redness (Figure 2). As shown by L^* (lower is darker; higher is brighter), leaf brightness was higher under WW_{180} and MW_{180} than $B_{20}G_{60}R_{100}$, $MW_{100}B_{50}R_{30}$, and $B_{60}G_{60}R_{60}$. As shown by a^* (lower is greener; higher is redder), leaves were greenest under WW_{180} and MW_{180} and reddest under $MW_{100}B_{50}R_{30}$, and $B_{60}G_{60}R_{60}$. As shown by b^* (lower is bluer; higher is yellower), leaves were yellower under WW_{180} and MW_{180} than the other treatments. The relative chlorophyll index (SPAD value) was 12–16% lower for plants grown under MW_{180} than the other treatments.

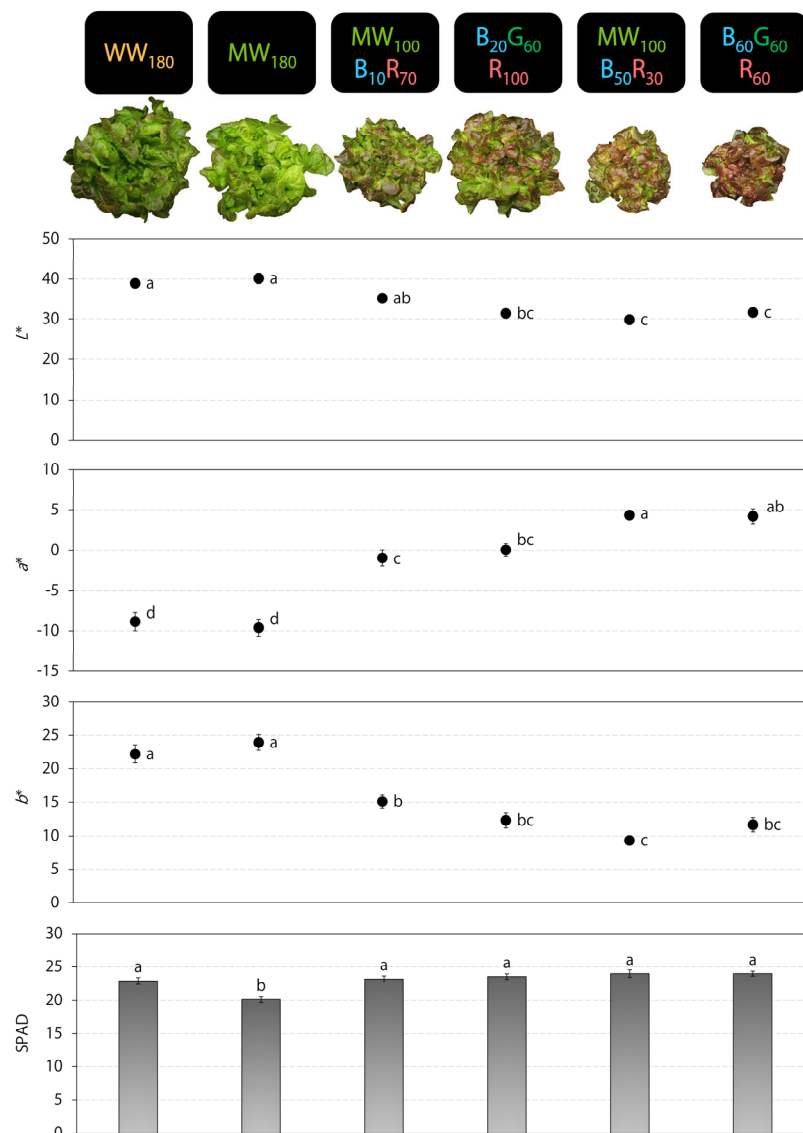


Figure 2. Leaf color indices ($L^*a^*b^*$) and relative chlorophyll index (SPAD value) of red-leaf lettuce ‘Rouxai’ grown under six indoor lighting treatments delivered by warm-white (WW), mint-white (MW), blue (B), green (G), and/or red (R) light-emitting diodes (LEDs) ($n = 20$). The number after each LED type is its photon flux density in $\mu\text{mol}\cdot\text{m}^{-2}\cdot\text{s}^{-1}$. For each parameter, values followed by different letters are statistically different ($\alpha = 0.05$).

2.3. Phenotypes Influenced by Blue Light

The six treatments in this study provided a wide range of blue photon flux densities, from 12 to $62 \mu\text{mol}\cdot\text{m}^{-2}\cdot\text{s}^{-1}$. Several major lettuce phenotypic parameters showed dose-

dependent relationships to the blue photon flux density (Figure 3). Increasing the blue photon flux density linearly decreased the shoot fresh and dry mass, leaf length and width, and plant diameter while increasing the leaf redness (as shown by a^*).

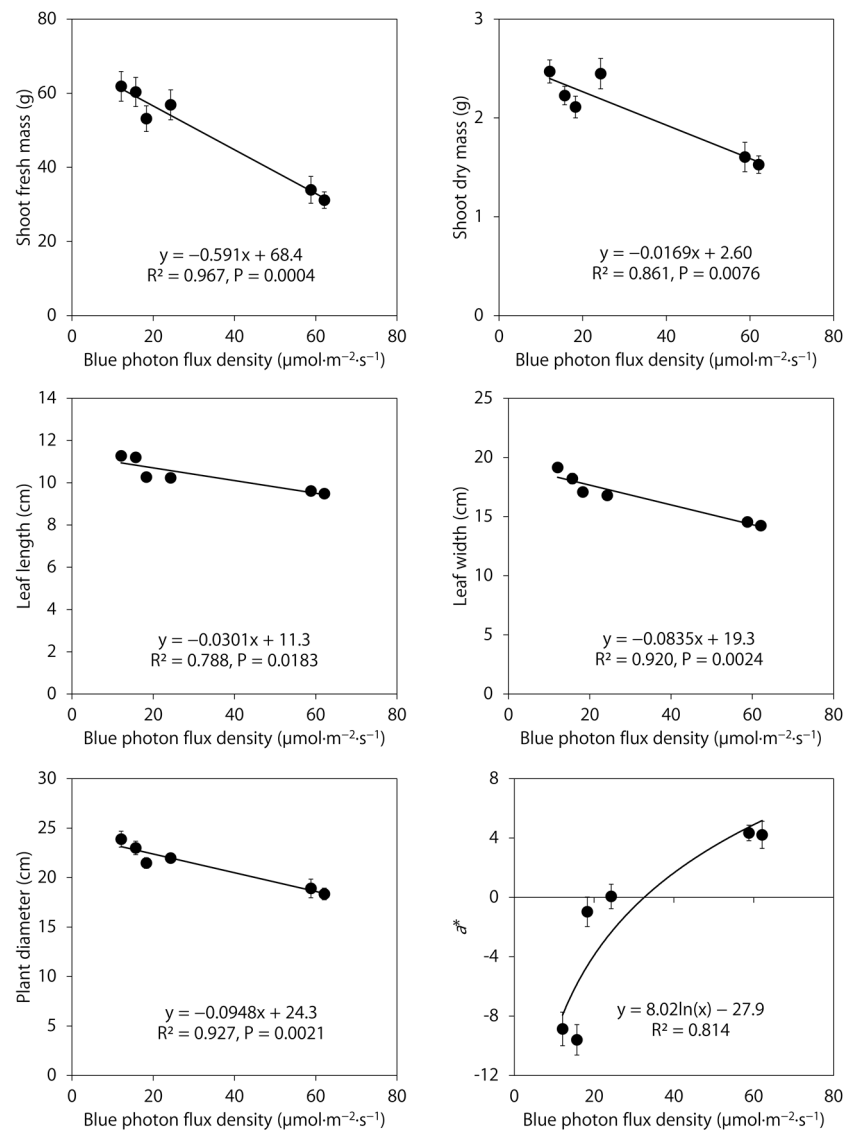


Figure 3. Relationships between the blue photon flux density and shoot biomass, morphology, and red leaf coloration parameters of red-leaf lettuce ‘Rouxai’ grown under six indoor lighting treatments delivered by warm-white, mint-white, blue, green, and/or red light-emitting diodes, which provided a range of blue photon flux densities ($n = 20$).

3. Discussion

In this study, indoor hydroponic red-leaf lettuce ‘Rouxai’ grew similarly under warm-white and mint-white LEDs, which provided similar blue fractions of 7% and 9%, respectively, but different green, red, and far-red fractions (Table 1). Low blue light was a signal to increase extension growth of lettuce ‘Rouxai’, irrespective of green and red light, which led to greater shoot growth [8]. Warm-white LEDs emitted more far-red photons (10%) than mint-white LEDs (3%), leading to red-to-far-red ratios of 5.3 and 8.1, respectively, and internal phytochrome photoequilibria of 0.661 and 0.722, respectively (Table 1). Despite these differences in spectra, warm-white and mint-white LEDs had comparable effects on lettuce growth (biomass), morphology (leaf size), and coloration. Lettuce shoot biomass was greatest under these two white LED types at least partly due to greater leaf expansion and canopy size, which increased light interception for photosynthesis. However, lettuce

appeared mostly green under the two white spectra and lacked red coloration, indicating low anthocyanin accumulation. Because high-energy blue photons induce rapid anthocyanin accumulation and enhance plant resilience in crops including red-leaf lettuce [17–19], the low blue fractions in the two white spectra could explain the lack of red leaf coloration. In this study, lettuce grown under broad spectra with higher blue photon flux densities had redder leaves. Similar to our results, partially substituting equalized-white light with blue light increased red leaf coloration and anthocyanin concentration of red-leaf lettuce ‘Red Butter’ [20].

The effects of 44% substitution of mint-white light with blue + red light on lettuce growth depended on the blue-to-red ratio. The lower substitute blue-to-red ratio of 1:7 changed the blue, green, red, and far-red photon flux densities by 2.6, −49.4, 47.8, and $-2.3 \mu\text{mol}\cdot\text{m}^{-2}\cdot\text{s}^{-1}$ (17%, −46%, 94%, and −37%), respectively (Table 1). At a blue photon flux density of 16–18 $\mu\text{mol}\cdot\text{m}^{-2}\cdot\text{s}^{-1}$, this substitution of green photons with red photons decreased lettuce shoot fresh mass by 12% (but not dry mass), decreased leaf length by 8%, intensified red leaf coloration, and increased chlorophyll concentration. In a separate study with a similar blue photon flux density, substituting 60 $\mu\text{mol}\cdot\text{m}^{-2}\cdot\text{s}^{-1}$ of green photons with red photons also decreased lettuce shoot fresh mass by 15% and leaf number but did not influence other parameters [8]. On the other hand, partial substitution of mint-white light with the higher blue-to-red ratio (5:3) changed the blue, green, red, and far-red photon flux densities by 43.1, −48.9, 7.9, and $-2.6 \mu\text{mol}\cdot\text{m}^{-2}\cdot\text{s}^{-1}$ (275%, −45%, 16%, and −42%), respectively (Table 1). This increased the blue photon flux density, which decreased lettuce shoot fresh and dry mass by 44% and 28%, respectively; decreased leaf number, leaf size, and canopy size; and increased red leaf coloration and chlorophyll concentration. Similarly, substituting green photons with blue photons decreased shoot mass and leaf expansion while increasing coloration and chlorophyll concentration of lettuce ‘Rex’ and ‘Rouxai’ and kale (*Brassica oleracea* var. *sabellica*) ‘Siberian’ [9].

We combined monochromatic blue + green + red LEDs to deliver similar 100 nm waveband flux densities of blue, green, red, and far-red light to the two mint-white + blue + red treatments. The former created three distinct peaks of narrowband radiation, whereas the latter created somewhat broader, more continuous photon distributions from the phosphor conversion of blue LEDs. Despite these spectral distribution differences, all measured lettuce phenotypes were similar when the integrated blue, green, red, and far-red photon wavebands were similar. However, narrowband green LEDs have a low efficacy ($0.54 \mu\text{mol}\cdot\text{J}^{-1}$ at full power), whereas mint-white LEDs emit green photons at a much higher efficacy ($1.52 \mu\text{mol}\cdot\text{J}^{-1}$ at full power) [15]. In addition, the color fidelity of plants was superior under mint-white + blue + red LEDs (CRI = 77–82) than their blue + green + red counterparts (CRI = 58–61) or mint-white LEDs alone (CRI = 63). The higher visual quality under mint-white + blue + red LEDs creates better working conditions and facilitates plant inspection for nutrient and physiological disorders and integrated pest management. Similarly, mint-white + red LEDs (3:1 or 9:11) delivered a higher CRI of 72–77 than blue + green + red LEDs (CRI = 56) or mint-white LEDs alone (CRI = 63) [15]. Lastly, warm-white LEDs are more ubiquitous and have a nearly perfect CRI of 97 but have a slightly lower efficacy ($1.28 \mu\text{mol}\cdot\text{J}^{-1}$ at full power) than mint-white LEDs, although both are considered white light.

We identified a dose-dependent inverse relationship between the blue photon flux density in a broad spectrum and the measured lettuce phenotypes in this study (Figure 3). The blue photon flux density appears to accurately predict these lettuce phenotypes, although these models could be further strengthened in future research by including additional broadband spectra with intermediate blue photon flux densities, especially between 25 and 60 $\mu\text{mol}\cdot\text{m}^{-2}\cdot\text{s}^{-1}$. In general, a broad spectrum with a higher blue photon flux density (in the range of 12–62 $\mu\text{mol}\cdot\text{m}^{-2}\cdot\text{s}^{-1}$) progressively decreased lettuce shoot biomass, leaf size, and canopy size but increased red leaf coloration. In a previous study, increasing the blue photon flux density in blue + green + red LEDs from 0 to 100 $\mu\text{mol}\cdot\text{m}^{-2}\cdot\text{s}^{-1}$ at a fixed photosynthetic photon flux density (PPFD) of 180 $\mu\text{mol}\cdot\text{m}^{-2}\cdot\text{s}^{-1}$ produced similar

results [8]. In contrast, increasing the blue photon flux density from 22 to 55 $\mu\text{mol}\cdot\text{m}^{-2}\cdot\text{s}^{-1}$ in a broad spectrum (from blue + green + red or warm-, neutral-, or cool-white LEDs) at a PPFD of 200 $\mu\text{mol}\cdot\text{m}^{-2}\cdot\text{s}^{-1}$ decreased dry mass and leaf area index of tomato (*Solanum lycopersicum*), but not other crops including green-leaf lettuce ‘Waldmann’s Green’ [21]. The four broad-spectrum treatments in that study had similarly high green fractions (41–48% of the PPFD), whereas the green fractions in this study and [8] were 32–33% of the PPFD in all treatments except for the mint-white LED treatment, in which 62% of the PPFD was of green light. The discrepancy in blue light responses could be at least partly attributed to potential blue and green light interactions. The inconsistent responses among studies could also be caused by different plant densities and maturities at harvest.

Although the effects of blue light on plant growth and morphology vary by species and spectral conditions such as the PPFD [22], increasing blue light in combined blue + red LEDs generally restricts lettuce extension growth, light capture, and biomass accumulation [23–25]. Cryptochromes 1 and 2 are photoreceptors that absorb blue light and regulate extension growth [26]. In *Arabidopsis thaliana*, PHYTOCHROME-INTERACTING FACTOR 4 (PIF4) and PIF5 are transcription factors that promote extension growth in the shade avoidance response [27]. Under low blue light, cryptochromes 1 and 2 interact with PIF4 and PIF5 to promote extension growth [28]. However, under sufficiently high blue light, cryptochromes 1 and 2 suppress the function of PIF4 while cryptochrome 2 and PIF5 are targeted for degradation [28]. A similar mechanism in lettuce could explain the reduced extension growth under broad spectra containing high blue light.

4. Materials and Methods

4.1. Plant Material and Propagation

We performed this experiment twice over time as a randomized complete block design in the Controlled-Environment Lighting Laboratory at Michigan State University (East Lansing, MI, USA). We rinsed and soaked rockwool cubes (AO 25/40, 25 × 25 × 40 mm; Grodan, Milton, ON, Canada) with deionized water, drained excess water from plastic trays, sowed one seed of red-leaf lettuce ‘Rouxai’ (Johnny’s Selected Seeds, Winslow, ME, USA) per cube, and covered them with transparent humidity domes. Seeds germinated under warm-white LED fixtures (CCT = 2700 K, PHYTOFY RL; OSRAM, Beverley, MA, USA) at a total photon flux density (400–799 nm) of 50 $\mu\text{mol}\cdot\text{m}^{-2}\cdot\text{s}^{-1}$ during the first 24 h at an air temperature setpoint of 20 °C. Based on visual assessment, we achieved a uniform seed germination rate of >95%. We then grew seedlings under 180 $\mu\text{mol}\cdot\text{m}^{-2}\cdot\text{s}^{-1}$ of warm-white light under a 20 h photoperiod at an air temperature setpoint of 22 °C until transplant on day 13. A total photon flux density of 180 $\mu\text{mol}\cdot\text{m}^{-2}\cdot\text{s}^{-1}$ was within the typical range delivered in commercial indoor vertical farms, while a 20 h photoperiod led to a daily light integral of 13 $\text{mol}\cdot\text{m}^{-2}\cdot\text{d}^{-1}$, which sufficed lettuce seedling growth [29]. The seedling trays sat on top of foam boards floating in tubs filled with water, in which the seedlings were subsequently transplanted.

After removing the humidity domes on day 4, we began lighting treatments and sub-irrigated the rockwool cubes as needed daily to submerge one fourth of the cube height in a nutrient solution with a pH of 5.7–5.9 and electrical conductivity of 1.2–1.4 $\text{dS}\cdot\text{m}^{-1}$. We prepared it in 18.9-L buckets by dissolving a 12.0N–1.7P–13.3K base fertilizer (12–4–16 RO Hydro FeED; JR Peters, Inc., Allentown, PA, USA) and magnesium sulfate (Epsom salt; Pennington Seed, Inc., Madison, GA, USA) sequentially in deionized water. The nutrient solution provided seedlings with the following nutrients (in $\text{mg}\cdot\text{L}^{-1}$): 125 N, 18 P, 139 K, 73 Ca, 49 Mg, 39 S, 1.7 Fe, 0.52 Mn, 0.56 Zn, 0.13 B, 0.47 Cu, and 0.13 Mo. We adjusted the nutrient solution pH with dry potassium bicarbonate and diluted (1:31) 95% to 98% sulfuric acid (J.Y. Baker, Inc., Phillipsburg, NJ, USA).

4.2. Lighting Treatments

On day 4, we transferred uniform lettuce seedlings to six broad-spectrum treatments. These treatments delivered the same total photon flux density of 180 $\mu\text{mol}\cdot\text{m}^{-2}\cdot\text{s}^{-1}$ under

a 20 h photoperiod (0200–2200 h), resulting in a daily light integral of $13 \text{ mol}\cdot\text{m}^{-2}\cdot\text{d}^{-1}$, which was sufficient to produce lettuce in the exponential growth phase [29,30]. Tunable multi-colored LED fixtures (PHYTOFY RL; OSRAM) delivered warm-white (WW₁₈₀) light, mint-white (MW₁₈₀) light, mint-white partially substituted with two ratios of blue + red light (MW₁₀₀B₁₀R₇₀ and MW₁₀₀B₅₀R₃₀), and combined monochromatic blue + green + red light with two ratios of blue + red light (B₂₀G₆₀R₁₀₀ and B₆₀G₆₀R₆₀). The number after each LED type indicates its photon flux density in $\mu\text{mol}\cdot\text{m}^{-2}\cdot\text{s}^{-1}$. During the setup of each lighting treatment, we took spectral scans at nine representative locations at plant canopy (46 cm below the LED fixtures) with a spectroradiometer (PS200; Apogee Instruments, Inc., Logan, UT, USA). We used the average photon flux density to adjust the fixture output in lighting control software (Spartan Control Software 2018 version 1; OSRAM) until the average was $\pm 3 \mu\text{mol}\cdot\text{m}^{-2}\cdot\text{s}^{-1}$ for each LED type. The spectral characteristics and distributions of the six lighting treatments are shown in Table 1 and Figure 4, respectively. The peak wavelengths of warm-white, mint-white, blue, green, and red LEDs were 639, 559, 449, 526, and 664 nm, respectively.

Table 1. Spectral characteristics of six broad-spectrum lighting treatments delivered by warm-white (WW), mint-white (MW), blue (B), green (G), and/or red (R) light-emitting diodes (LEDs).

| Lighting Treatment | WW ₁₈₀ ¹ | MW ₁₈₀ | MW ₁₀₀ B ₁₀ R ₇₀ | B ₂₀ G ₆₀ R ₁₀₀ | MW ₁₀₀ B ₅₀ R ₃₀ | B ₆₀ G ₆₀ R ₆₀ |
|--------------------|---|-------------------|---|--|---|---|
| | Photon flux density and percentage of each waveband ($\mu\text{mol}\cdot\text{m}^{-2}\cdot\text{s}^{-1}$) | | | | | |
| B ² | 12.1 (7%) | 15.7 (9%) | 18.3 (10%) | 24.3 (13%) | 58.8 (33%) | 62.1 (35%) |
| G | 51.9 (29%) | 107.7 (60%) | 58.3 (33%) | 58.9 (32%) | 58.8 (33%) | 58.8 (33%) |
| R | 98.4 (54%) | 50.6 (28%) | 98.4 (55%) | 99.1 (54%) | 58.5 (32%) | 57.5 (32%) |
| FR | 18.6 (10%) | 6.2 (3%) | 3.9 (2%) | 1.2 (1%) | 3.6 (2%) | 0.7 (0%) |
| | Integrated photon flux density ($\mu\text{mol}\cdot\text{m}^{-2}\cdot\text{s}^{-1}$) | | | | | |
| PPFD ³ | 162.4 | 174.0 | 175.0 | 182.3 | 176.1 | 178.4 |
| TPFD | 181.0 | 180.2 | 179.0 | 183.5 | 179.7 | 179.1 |
| YFPD ⁴ | 148.9 | 154.1 | 156.8 | 156.5 | 150.1 | 146.1 |
| | Light ratios and metrics | | | | | |
| B:R | 0.12 | 0.31 | 0.19 | 0.25 | 1.01 | 1.08 |
| R:FR | 5.3 | 8.1 | 25.0 | 85.5 | 16.3 | 84.6 |
| Ippe ⁴ | 0.661 | 0.722 | 0.814 | 0.843 | 0.771 | 0.813 |
| CRI ⁵ | 97 | 63 | 82 | 58 | 77 | 61 |

¹ The number after each LED type is its photon flux density in $\mu\text{mol}\cdot\text{m}^{-2}\cdot\text{s}^{-1}$. ² Each 100 nm waveband is defined as follows: B, 400–499 nm; G, 500–599 nm; R, 600–699 nm; and far red (FR), 700–799 nm. ³ The photosynthetic photon flux density (PPFD, 400–699 nm) and total photon flux density (TPFD, 400–799 nm) differed in the inclusion of far-red (FR) light. ⁴ The yield photon flux density (YFPD, 300–799 nm) and internal phytochrome photoequilibrium (IPPE) were calculated following [31,32], respectively. ⁵ The color rendering index (CRI) was calculated with the OSRAM Sylvania LED ColorCalculator.

4.3. Hydroponic System and Environment

On day 13, we transplanted lettuce seedlings into the 36-cell foam rafts ($60.9 \times 121.9 \times 2.5$ cm; Beaver Plastics, Ltd.; Acheson, AB, Canada) floating on top of nutrient solutions in flood tables ($1.22 \times 0.61 \times 0.18$ m; Active Aqua AAHR24W; Hydrofarm, Petaluma, CA, USA) of a deep flow technique hydroponic system. At a planting density of $48.4 \text{ plants}\cdot\text{m}^{-2}$, plant centers were 20.3 cm apart horizontally and 14.6 cm apart diagonally. The nutrient solutions were constantly recirculated with water pumps and aerated with air stone discs (20.3×2.5 cm; Active Aqua AS8RD; Hydrofarm), which were submerged in three reservoirs and connected to external air pumps (Active Aqua AAPA70L; Hydrofarm). The nutrient solutions contained the same two-part fertilizers in deionized water as for seedlings and provided the following initial nutrients at transplant (in $\text{mg}\cdot\text{L}^{-1}$): 150 N, 22 P, 166 K, 88 Ca, 58 Mg, 47 S, 2.1 Fe, 0.63 Mn, 0.68 Zn, 0.15 B, 0.56 Cu, and 0.15 Mo.

From transplant to harvest, we measured the nutrient solution pH, electrical conductivity, and temperature daily with a pH and electrical conductivity meter (HI9814; Hanna Instruments, Woonsocket, RI, USA). Each of these parameters was similar among the three reservoirs, which were used for the six lighting treatments, throughout the two replications

(Figure 5). Whenever the pH was <5.1 , we used potassium bicarbonate to raise the nutrient solution pH to 5.6–5.9 until day 28, after which we did not adjust it to observe the effects of plant nutrient uptake. Because 98% of the total nitrogen in the base fertilizer was in the nitrate form, maturing lettuce increased the nutrient solution pH. We replenished three reservoirs with deionized water periodically to ensure the water pumps were fully submerged in the reservoirs but did not provide additional fertilizers. Consequently, the nutrient solution electrical conductivity decreased gradually from 1.8 to 1.9 $\text{dS}\cdot\text{m}^{-1}$ at transplant to 1.5 to 1.7 $\text{dS}\cdot\text{m}^{-1}$ at harvest.

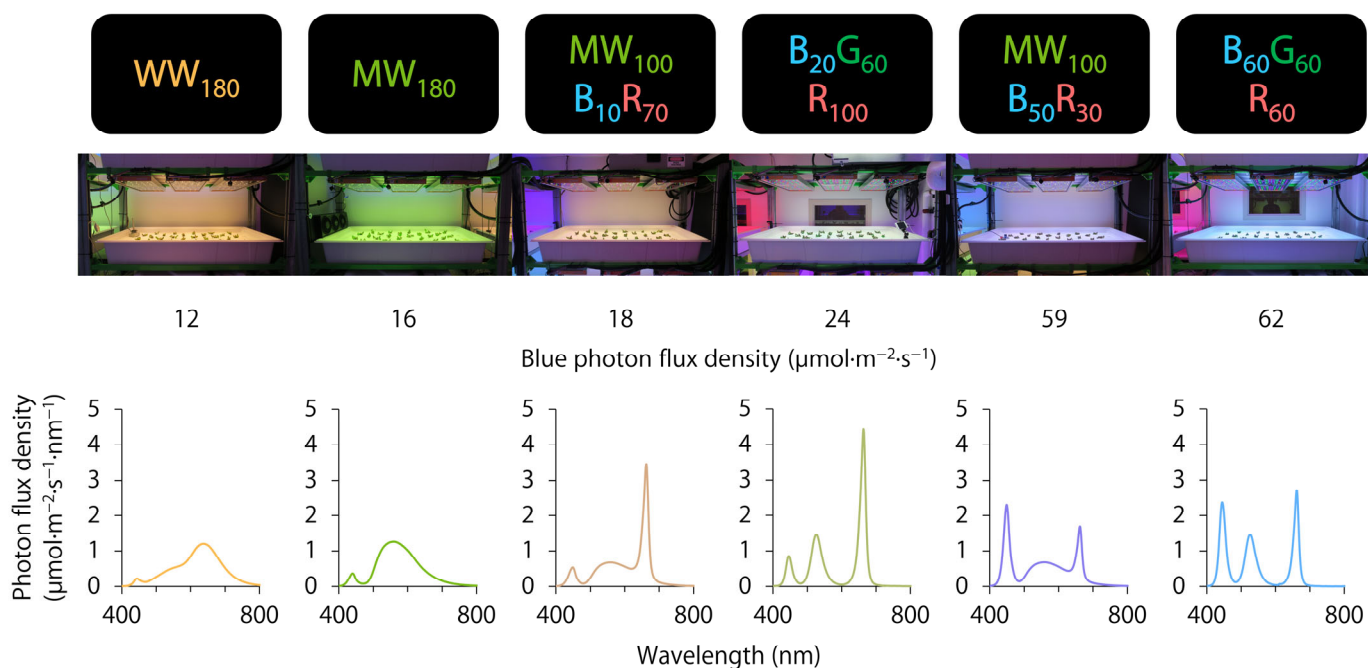


Figure 4. Photos and spectral distributions of six indoor lighting treatments delivered by warm-white (WW), mint-white (MW), blue (B), green (G), and/or red (R) light-emitting diodes (LEDs). The number after each LED type is its photon flux density in $\mu\text{mol}\cdot\text{m}^{-2}\cdot\text{s}^{-1}$.

A ventilation and air-conditioning unit (HBH030A3C20CRS; Heat Controller, LLC., Jackson, MI, USA), which was connected to a wireless thermostat controller (Honeywell International, Inc., Morris Plains, NJ, USA), maintained a constant air temperature setpoint of 22 °C. Plants were grown at the ambient CO_2 concentration. We monitored the environment with a temperature and relative humidity sensor (HMP110; Vaisala, Inc., Louisville, CO, USA) and a CO_2 sensor (GMD20; Vaisala, Inc.). Sensors were wired to a datalogger (CR1000; Campbell Scientific, Inc., Logan, UT, USA) that recorded hourly means of 10 s intervals (Figure 6). The mean air temperature, CO_2 concentration, and relative humidity (mean \pm SD) were 22.4 ± 0.6 °C, 410 ± 50 $\mu\text{mol}\cdot\text{mol}^{-1}$, and $34\% \pm 10\%$, respectively, in replication 1 and 22.5 ± 0.6 °C, 398 ± 35 $\mu\text{mol}\cdot\text{mol}^{-1}$, and $35\% \pm 7\%$, respectively, in replication 2.

4.4. Data Collection and Analysis

On day 30 and 33 in the two consecutive replications, we harvested and conducted destructive measurements on eight randomly selected plants from each lighting treatment. For each plant, we measured shoot fresh mass with a top-loading balance (GX-1000; A&D Store, Inc., Wood Dale, IL, USA), the number of leaves longer than 3 cm, plant diameter (the longest horizontal distance between plant edges), and the length and width of the sixth most mature true leaf. At three random locations on recently matured leaves of each plant, we also measured the International Commission on Illumination $L^*a^*b^*$ color space values with a color reader (Chroma Meter CR-400; Konica Minolta Sensing, Inc., Chiyoda, Tokyo,

Japan) and the relative chlorophyll index (SPAD value) with a chlorophyll meter (SPAD-502; Konica Minolta Sensing, Inc.). These pigmentation measurements targeted unshaded interveinal leaf tissue. Subsequently, we placed each plant in a paper bag, dried it for ≥ 5 d at 60 °C in a forced air drying oven (Blue M, Blue Island, IL, USA), and measured shoot dry mass. In addition, we photographed a representative plant from each lighting treatment from overhead to document crop appearance (Figures 1 and 2). We analyzed plant data with SAS (version 9.4; SAS Institute, Inc., Cary, NC, USA) using the PROC MEANS, PROC MIXED, and PROC GLIMMIX procedures and Tukey's honestly significant difference test ($\alpha = 0.05$). We also performed regression analysis between the blue photon flux density and plant parameters with Microsoft Excel (Microsoft, Redmond, WA, USA). All data were pooled for analysis because of the non-significance of the treatment \times replication interaction term ($p > 0.05$) and/or similar treatment trends between replications.

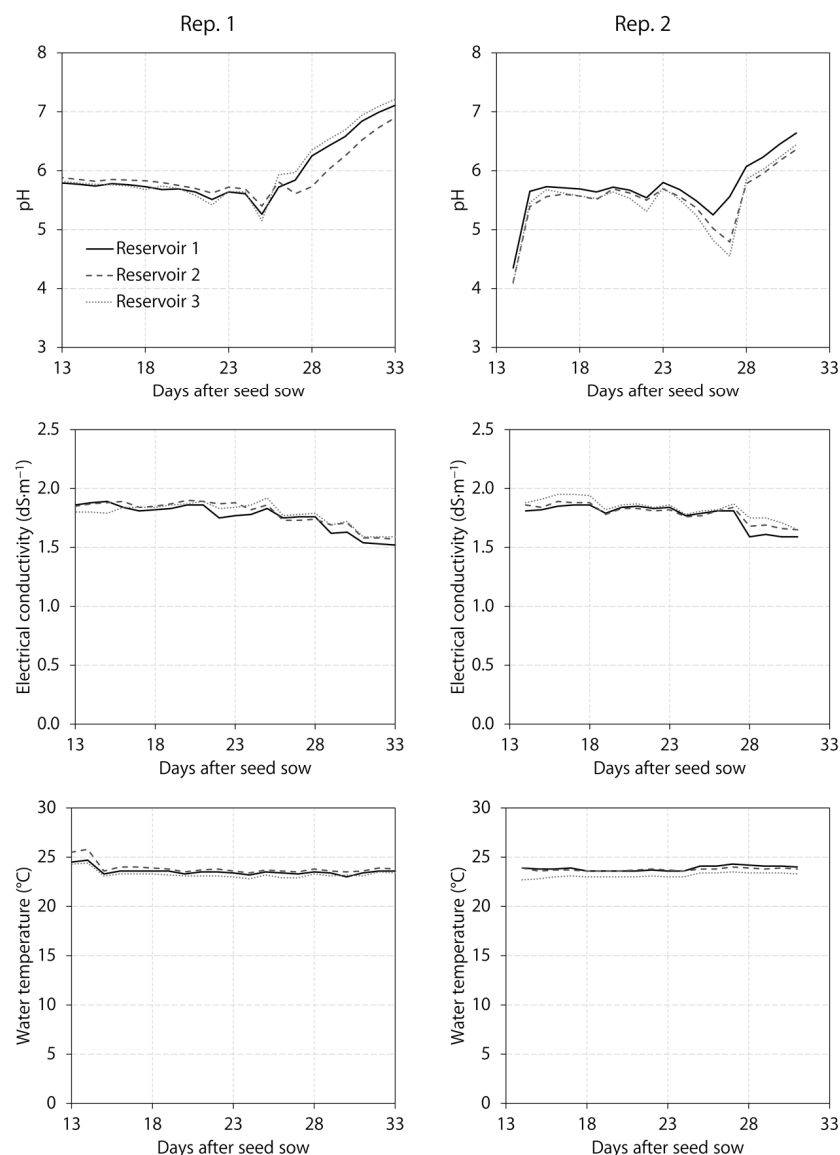


Figure 5. Nutrient solution pH, electrical conductivity, and temperature of three reservoirs used throughout two experimental replications (Rep.) for six indoor lighting treatments delivered by warm-white, mint-white, blue, green, and/or red light-emitting diodes (LEDs). Reservoir 1 was for the two blue + green + red LED treatments. Reservoir 2 was for the mint-white LED treatment. Reservoir 3 was for the warm-white LED treatment and the two mint-white + blue + red LED treatments.

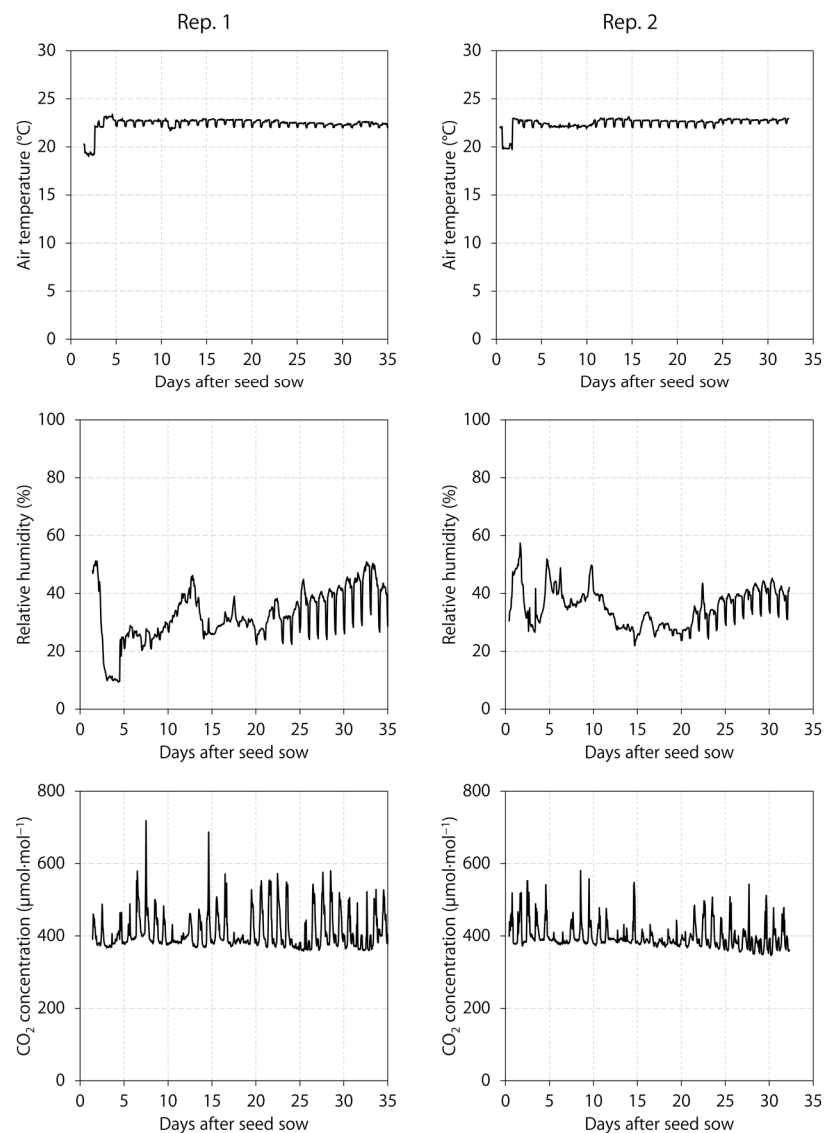


Figure 6. Air temperature, relative humidity, and CO₂ concentration throughout two experimental replications (Rep.) of the growth room housing six indoor lighting treatments delivered by warm-white, mint-white, blue, green, and/or red light-emitting diodes. The CO₂ peaks were caused by people inside the growth room.

5. Conclusions

Warm-white and mint-white LEDs with distinctly different broad spectra had similar effects on indoor hydroponic lettuce biomass, morphological traits, and pigmentation. When a phosphor-converted broad spectrum (mint white) was partially substituted with blue + red light, the change in the blue photon flux density primarily determined the plant phenotypic responses. Lettuce grew similarly under mint-white LEDs partially substituted with blue + red LEDs and blue + green + red LEDs that delivered similar photon flux densities of 100 nm blue, green, and red wavebands. Lastly, the blue photon flux density in the six broad spectra tested was an accurate predictor of lettuce growth and coloration.

Author Contributions: Conceptualization, Q.M. and E.S.R.; methodology, Q.M. and E.S.R.; software, Q.M.; validation, Q.M. and E.S.R.; formal analysis, Q.M.; investigation, Q.M.; resources, E.S.R.; data curation, Q.M. and E.S.R.; writing—original draft preparation, Q.M.; writing—review and editing, Q.M. and E.S.R.; visualization, Q.M.; supervision, E.S.R.; project administration, E.S.R.; funding acquisition, E.S.R. All authors have read and agreed to the published version of the manuscript.

Funding: This research was funded by Michigan State University AgBioResearch, Project GREEN GR17-072, and USDA National Institute of Food and Agriculture, Hatch project 192266.

Data Availability Statement: The datasets used and/or analyzed in this manuscript are available from the first corresponding author on reasonable request by e-mail.

Acknowledgments: The authors thank David Hamby, Rodrigo Pereyra, Charles Brunault, Alan Sarkisian, and Dorian Spero from OSRAM Innovation for lighting support; Nathan Kelly for experimental assistance; Steve Brooks for technical assistance; Randy Beaudry, Dan Brainard, and Roberto Lopez for instruments; and Grodan and JR Peters, Inc. for material donations.

Conflicts of Interest: The authors declare no conflict of interest.

References

1. Liu, J.; van Iersel, M.W. Photosynthetic physiology of blue, green, and red light: Light intensity effects and underlying mechanisms. *Front. Plant Sci.* **2021**, *12*, 328. [[CrossRef](#)] [[PubMed](#)]
2. Zhen, S.; Haidekker, M.; van Iersel, M.W. Far-red light enhances photochemical efficiency in a wavelength-dependent manner. *Physiol. Plant.* **2019**, *167*, 21–33. [[CrossRef](#)]
3. Zhen, S.; Bugbee, B. Far-red photons have equivalent efficiency to traditional photosynthetic photons: Implications for redefining photosynthetically active radiation. *Plant Cell Environ.* **2020**, *43*, 1259–1272. [[CrossRef](#)] [[PubMed](#)]
4. Zhen, S.; van Iersel, M.; Bugbee, B. Why far-red photons should be included in the definition of photosynthetic photons and the measurement of horticultural fixture efficacy. *Front. Plant Sci.* **2021**, *12*, 1158. [[CrossRef](#)] [[PubMed](#)]
5. Briggs, W.R.; Huala, E. Blue-light photoreceptors in higher plants. *Annu. Rev. Cell Dev. Biol.* **1999**, *15*, 33–62. [[CrossRef](#)]
6. Sharrock, R.A. The phytochrome red/far-red photoreceptor superfamily. *Gen. Biol.* **2008**, *9*, 230. [[CrossRef](#)]
7. Folta, K.M.; Maruhnich, S.A. Green light: A signal to slow down or stop. *J. Exp. Bot.* **2007**, *58*, 3099–3111. [[CrossRef](#)]
8. Meng, Q.; Boldt, J.; Runkle, E.S. Blue radiation interacts with green radiation to influence growth and predominantly controls quality attributes of lettuce. *J. Am. Soc. Hortic. Sci.* **2020**, *145*, 75–87. [[CrossRef](#)]
9. Meng, Q.; Kelly, N.; Runkle, E.S. Substituting green or far-red radiation for blue radiation induces shade avoidance and promotes growth in lettuce and kale. *Environ. Exp. Bot.* **2019**, *162*, 383–391. [[CrossRef](#)]
10. Franklin, K.A. Shade avoidance. *New Phytol.* **2008**, *179*, 930–944. [[CrossRef](#)]
11. Kusuma, P.; Pattison, P.M.; Bugbee, B. From physics to fixtures to food: Current and potential LED efficacy. *Hortic. Res.* **2020**, *7*, 56. [[CrossRef](#)] [[PubMed](#)]
12. Zheng, L.; He, H.; Song, W. Application of light-emitting diodes and the effect of light quality on horticultural crops: A review. *HortScience* **2019**, *54*, 1656–1661. [[CrossRef](#)]
13. Bispo, A.G., Jr.; Saraiva, L.F.; Lima, S.A.; Pires, A.M.; Davolos, M.R. Recent prospects on phosphor-converted LEDs for lighting, displays, phototherapy, and indoor farming. *J. Lumin.* **2021**, *237*, 118167. [[CrossRef](#)]
14. Cope, K.R.; Bugbee, B. Spectral effects of three types of white light-emitting diodes on plant growth and development: Absolute versus relative amounts of blue light. *HortScience* **2013**, *48*, 504–509. [[CrossRef](#)]
15. Park, Y.; Runkle, E.S. Spectral effects of light-emitting diodes on plant growth, visual color quality, and photosynthetic photon efficacy: White versus blue plus red radiation. *PLoS ONE* **2018**, *13*, e0202386. [[CrossRef](#)]
16. Chen, X.L.; Xue, X.Z.; Guo, W.Z.; Wang, L.C.; Qiao, X.J. Growth and nutritional properties of lettuce affected by mixed irradiation of white and supplemental light provided by light-emitting diode. *Sci. Hortic.* **2016**, *200*, 111–118. [[CrossRef](#)]
17. Dou, H.; Niu, G.; Gu, M.; Masabni, J.G. Effects of light quality on growth and phytonutrient accumulation of herbs under controlled environments. *Horticulturae* **2017**, *3*, 36. [[CrossRef](#)]
18. Lazzarin, M.; Meisenburg, M.; Meijer, D.; Van Ieperen, W.; Marcelis, L.F.M.; Kappers, I.F.; Van der Krol, A.R.; van Loon, J.J.A.; Dicke, M. LEDs make it resilient: Effects on plant growth and defense. *Trends Plant Sci.* **2021**, *26*, 496–508. [[CrossRef](#)]
19. Lee, J.S.; Lim, T.G.; Yong, H.K. Growth and phytochemicals in lettuce as affected by different ratios of blue to red LED radiation. *Acta Hortic.* **2014**, *1037*, 843–848.
20. Li, Y.; Wu, L.; Jiang, H.; He, R.; Song, S.; Su, W.; Liu, H. Supplementary far-red and blue lights influence the biomass and phytochemical profiles of two lettuce cultivars in plant factory. *Molecules* **2021**, *26*, 7405. [[CrossRef](#)]
21. Snowden, M.C.; Cope, K.R.; Bugbee, B. Sensitivity of seven diverse species to blue and green light: Interactions with photon flux. *PLoS ONE* **2016**, *11*, e0163121. [[CrossRef](#)]
22. Huché-Thélier, L.; Crespel, L.; Le Gourrierec, J.; Morel, P.; Sakr, S.; Leduc, N. Light signaling and plant responses to blue and UV radiations—Perspectives for applications in horticulture. *Environ. Exp. Bot.* **2016**, *121*, 22–38. [[CrossRef](#)]
23. Kang, W.H.; Park, J.S.; Park, K.S.; Son, J.E. Leaf photosynthetic rate, growth, and morphology of lettuce under different fractions of red, blue, and green light from light-emitting diodes (LEDs). *Hortic. Environ. Biotechnol.* **2016**, *57*, 573–579. [[CrossRef](#)]
24. Son, K.H.; Oh, M.M. Growth, photosynthetic and antioxidant parameters of two lettuce cultivars as affected by red, green, and blue light-emitting diodes. *Hortic. Environ. Biotechnol.* **2015**, *56*, 639–653. [[CrossRef](#)]
25. Wang, J.; Lu, W.; Tong, Y.; Yang, Q. Leaf morphology, photosynthetic performance, chlorophyll fluorescence, stomatal development of lettuce (*Lactuca sativa* L.) exposed to different ratios of red light to blue light. *Front. Plant Sci.* **2016**, *7*, 250. [[CrossRef](#)] [[PubMed](#)]

26. Yu, X.; Liu, H.; Klejnot, J.; Lin, C. The cryptochrome blue light receptors. *Arab. Book* **2010**, *8*, e0135. [[CrossRef](#)] [[PubMed](#)]
27. Kunihiro, A.; Yamashino, T.; Nakamichi, N.; Niwa, Y.; Nakanishi, H.; Mizuno, T. Phytochrome-interacting factor 4 and 5 (PIF4 and PIF5) activate the homeobox *ATHB2* and auxin-inducible *IAA29* genes in the coincidence mechanism underlying photoperiodic control of plant growth of *Arabidopsis thaliana*. *Plant Cell Physiol.* **2011**, *52*, 1315–1329. [[CrossRef](#)]
28. Pedmale, U.V.; Huang, S.S.C.; Zander, M.; Cole, B.J.; Hetzel, J.; Ljung, K.; Reis, P.A.; Sridevi, P.; Nito, K.; Nery, J.R.; et al. Cryptochromes interact directly with PIFs to control plant growth in limiting blue light. *Cell* **2016**, *164*, 233–245. [[CrossRef](#)]
29. Meng, Q.; Runkle, E.S. Growth responses of red-leaf lettuce to temporal spectral changes. *Front. Plant Sci.* **2020**, *11*, 571788. [[CrossRef](#)] [[PubMed](#)]
30. Kelly, N.; Choe, D.; Meng, Q.; Runkle, E.S. Promotion of lettuce growth under an increasing daily light integral depends on the combination of the photosynthetic photon flux density and photoperiod. *Sci. Hortic.* **2020**, *272*, 109565. [[CrossRef](#)]
31. Sager, J.C.; Smith, W.O.; Edwards, J.L.; Cyr, K.L. Photosynthetic efficiency and phytochrome photoequilibria determination using spectral data. *Trans. Am. Soc. Agric. Eng.* **1988**, *31*, 1882–1889. [[CrossRef](#)]
32. Kusuma, P.; Bugbee, B. Improving the predictive value of phytochrome photoequilibrium: Consideration of spectral distortion within a leaf. *Front. Plant Sci.* **2021**, *12*, 596943. [[CrossRef](#)] [[PubMed](#)]

Disclaimer/Publisher’s Note: The statements, opinions and data contained in all publications are solely those of the individual author(s) and contributor(s) and not of MDPI and/or the editor(s). MDPI and/or the editor(s) disclaim responsibility for any injury to people or property resulting from any ideas, methods, instructions or products referred to in the content.